Electrochemical Machining of Aluminium Metal Matrix Composites

Article *in* Surface Engineering and Applied Electrochemistry · July 2018

DOI: 10.3103/S1068375518040087

2 authors:

Rajesh Jesudoss Hynes
Mepco Schlenk Engineering College
146 PUBLICATIONS **2,524** CITATIONS

R. Kumar
Eritrea Institute of Technology
49 PUBLICATIONS **923** CITATIONS

ISSN 1068-3755, Surface Engineering and Applied Electrochemistry, 2018, Vol. 54, No. 4, pp. 367–373. © Allerton Press, Inc., 2018.

Electrochemical Machining of Aluminium Metal Matrix Composites[1]

N. Rajesh Jesudoss Hynes[a] **and R. Kumar**[b, *]
[a] Department of Mechanical Engineering, Mepco Schlenk Engineering College, Sivakasi, Tamilnadu, 626 005 India
[b] Department of Mechanical Engineering, Vels Institute of Science, Technology & Advanced Studies, Chennai, Tamilnadu, 600 117 India
*e-mail: mepcokumar@gmail.com

Received August 2, 2017; in final form, December 26, 2017

Abstract—High performance aluminium based metal matrix composites possess low machinability characteristic. Electrochemical machining (ECM) is one of the advanced machining processes, used for machining of these newly developed exotic materials. This article critically reviews the research work on experimental investigations on ECM of aluminium matrix composites. Besides, recently developed techniques such as abrasive assisted electrochemical machining, electrochemical grinding, electrochemical micromachining, and electrochemical drilling are explored in the processing of aluminium metal matrix composites.

Keywords: electrochemical machining, process variants, process parameters, aluminium metal matrix, applications

DOI: 10.3103/S1068375518040087

INTRODUCTION

When compared to unreinforced alloys, aluminium metal matrix composites (AMMCs) are widely used in the applications of industries such as aerospace, automobile, defence, etc., because of certain significant properties like high strength-to-weight ratio, high stiffness, and high hardness, low wear rate and low coefficient of thermal expansion [1–4]. Generally, AMMCs are reinforced with some ceramic abrasive particles, which leads to abrasive action during machining. When machining of AMMCs is done with conventional techniques, then high tool wear is reported [5], resulting in the decline of the surface integrity of the material [6]. Machinability of composites is reduced while performing the traditional machine operations such as turning, milling, threading, etc. because those are hard-to-machine materials [7, 8]. In the traditional method, heat is generated during machining at the interface of tool and chip, which influences the surface integrity of the workpiece [9]. Machining cost also increases in the conventional machine to process hard particles reinforced AMMCs [10]. Many researchers reported the machining of metal matrix composites by unconventional machining processes. Laser beam machining and electrical discharge machining (EDM) provide more sub-surface damage to the workpiece than electrochemical machining (ECM) [11]. Among the unconventional techniques, ECM is the most significant one that could be employed for machining hard or difficult to cut materials [12, 13]. In this process, metal is removed from the electrically conductive workpiece by controlled dissolution. Here, tool and workpiece are considered as cathode and anode, respectively; both are separated by an electrolyte solution. It is mainly used for the manufacturing the complex shape components for automotive, aerospace, defence, medical and electronics industries such as engine castings, non-circular holes, bearing cages, forging dies and moulds, turbine blades, artillery projectiles, and surgical implants, etc. [14]. Besides, there are some important merits of ECM such as no stress, no burrs, longer tool life, damage-free machined surface.

ECM PROCESS

At the beginning of the XX century, some researchers suggested employing this principle as the base for the application of anodic material removal as a technique for machining hard materials. In the 1950s–1970s, several applications of ECM in the aerospace industries and tool manufacturing industries began in the USSR and in Western Europe. But only in 1959, for the first time, the Anocut Engineering Company, USA, introduced the traditional model of ECM, using direct current for the production run equipment. ECM is an unconventional machining process, which acts as a good alternative for producing three-dimensional complex shape components.

Principle

ECM is a process in which the removal of metal from the workpiece takes place by the controlled anodic dissolution, according to the laws of electro-

---

[1] The article is published in the original.

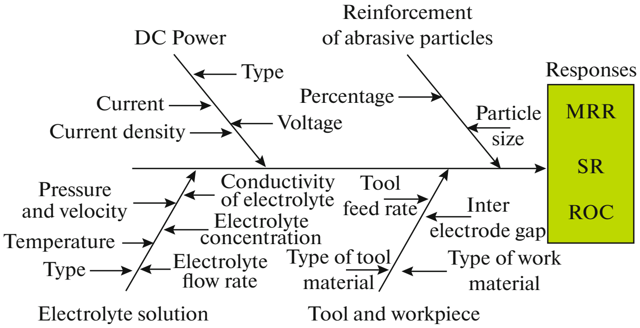

Fig. 1. Cause and effect analysis of ECM.

chemistry [15–18]. It is the reverse of deposition of material as in electroplating process and is used only for electrically conductive materials. In the gap in between the workpiece (anode) and tool (cathode) the electrolyte solution is allowed to flow at a high velocity.

Process Description

When a low voltage and high density electric current is allowed to pass through the electrolyte solution, the tool (cathode) is moved towards the anode in an accurate path, so as to remove the metal from the workpiece [19–22]. As a result of electrolysis, the metal gets removed from the anode and hydrogen is generated at the cathode. Further, no other reaction is produced at the electrodes [23]. An electrolyte solution is a concentrated salt which is not consumed during the process. This solution is passed through the inter-electrode gap in order to remove the machining waste and to reduce the heat generation. The pump and filter are required to pump the electrolyte at high velocity and to remove the sludge from the circulating electrolyte solution. ECM process continues until the required shape and dimension are obtained.

Process Parameters

Figure 1 shows the causes and effect diagram on the effect of the process parameters during ECM. The following are the most significant process parameters which are considered during ECM:

(i) Applied voltage
(ii) Current
(iii) Tool feed rate
(iv) Inter-electrode gap
(v) Electrolyte concentration
(vi) Electrolyte flow rate
(vii) Percentage of reinforcement

The rate of anodic dissolution is the amount of material disintegration that occurs during ECM at a particular time period. According to the laws of Michael Faraday, the current is a direct measure of the electrochemical reaction, which, in turn, depends on the voltage applied. An expression for material deposited or dissolved is derived from the laws of Michael Faraday as given in equation (1):

$$\mathrm{MRR} = \frac{\eta IE}{\mathrm{F}}, \quad (1)$$

where MRR: material removal rate in (g/min); η: current efficiency (%); I: current (A); E: electrochemical equivalent (g); F: Faraday's constant, i.e. 96500 A.s.

It is recommended that the applied current density should be in a range of 20 to 200 A/cm^2 for an effective material removal rate. The supplied voltage could be provided in a range of 10–25 volts [24]. Depending upon the material to be machined, the electrolyte is selected. In this process, the electrolyte is used in any form such as acidic, basic and neutral aqueous solution [25]. Table 1 shows the overview of the selection of various process parameters of ECM.

The researchers in [26] investigated the machining of a metal matrix composite in ECM. In this process, the authors used the inter-electrode gap in a range of 0.025–0.75 mm; hence 0.05 mm tolerance has resulted. They varied the current density in a range of 1–10 A/cm^2 and found that the current density 2.5 A/cm^2 was a better choice. Most commonly used electrolytes in ECM for machining of metal matrix composites are sodium nitrate ($NaNO_3$), sodium chloride (NaCl), potassium nitrate (KNO_3) and potassium chloride (KCl). Tool design is crucial for modelling of ECM [27]. By means of the finite element method, the tool shape could be designed in accordance with the geometry of the workpiece [28]. Most commonly used tool materials are copper, tungsten, tungsten carbide and titanium [29].

An increased tool feed rate reduces the gap between the tool and the workpiece which, in turn, leads to increasing the current density. Hence it accelerates the anodic dissolution and an eventual increase in the MRR and decreases the surface roughness (SR). The MRR is the amount of the material deposited or dissolved per unit of time and it is expressed in grams per unit time. It is mathematically presented in equation (1). The SR is a measure of the texture of a machined surface. Increasing the electrolyte concentration and the electrolyte flow rate leads to an increase in the MRR. High electrolyte concentration speeds up the production of ions from the material, which leads to a higher MRR. Moreover, when increasing the applied voltage at that moment, an increased current density at the gap results in higher anodic dissolution. It may be attributed to thin salt films produced at the work surface, which decreases the SR value [30]. Increasing the applied voltage and the electrolyte flow rate over a certain limit, results in a higher SR in the machined workpiece. At the beginning of the increase of the electrolyte flow rate, a high turbulence effect is observed resulting in the decline of the SR [31].

Table 1. Overview on selection of process parameters

Sl. No.	Research group	Variation of process parameters in ECM							
		Voltage	Current	Tool feed rate	Electrolyte	Electrolyte concentration	Electrolyte flow rate	Reinforcement	Inter electrode gap
		V	A	mm/min	–	g/L	L/min	wt %	mm
1	Senthilkumar et al. [38]	5–15	–	0.2–0.6	NaCl	30–100	5	5–15	0.3
2	Senthilkumar et al. [41]	12–16	–	0.2–1	$NaNO_3$	10–30	5–9	–	–
3	Rao et al. [45]	12–20	–	0.2–1	NaCl	10–30	–	2.5–7.5	–
4	Sankar et al. [49]	8–14	60–240	0.4–0.6	NaCl	–	–	5–15	–
5	Solaiyappan et al. [50]	10–26	205–265	0.2–1	NaCl	100–220	7–15	–	0.1–0.5

It is reported that when increasing the electrolyte concentration, the current density at the inter-electrode gap also tends to increase [32]. Resulted formation of pits on the surface of the machined workpiece continues until the pits overlap in order to achieve a smooth surface finish. Besides, enhancing the percentage of reinforcement particles in the metal matrix leads to the reduction in electrical conductivity of the anode (workpiece), since the reinforced particles have lower electrical conductivity than the metal matrix. Raising the process parameters such as applied voltage and electrolyte concentration increases the response of the radial over cut (ROC). The ROC is defined as half the difference of the diameter of the hole produced to the diameter of the tool. But this response reduces with the increase in the tool feed rate and in the percentage of reinforcement in the matrix. Thus, the MRR, SR, and ROC were found to decline at a higher percentage of reinforcement in the metal matrix.

PROCESS VARIANTS

Abrasive Assisted Electrochemical Machining

Sankar et al. [33] machined aluminium (Al)-B_4C-graphite hybrid composite by the abrasive assisted electrochemical machining (AECM). In that research, they used a cylindrically shaped copper piece as tool and abrasive as SiC particles of 50 μm. AECM differs from ECM by the combined action of anodic dissolution and mechanical abrasion to remove the metal from the workpiece. So, it was reported that the AECM process could produce more MRR than conventional electrochemical machining. Figure 2 shows the irregular workpiece surface, which leads to enhanced SR and also a few corroded particles that remain on the surface of the workpiece, produced during anodic dissolution. Figure 3 shows the surface of the regular workpiece produced on the machined surface by using AECM and it reveals that the corroded particles were effectively removed from the workpiece surface. Due to that, the improved surface finish was obtained when compared to that after machining of composites without abrasive particles.

Electrochemical Grinding

Goswami et al. [34] investigated the machining of Al-Al_2O_3 interpenetrating phase composite by using the electrochemical grinding (ECG). They considered such process parameters as applied voltage, depth of cut, electrolyte concentration, electrolyte flow rate, and the performance parameters such as MRR, SR, and cutting forces. They studied the effect of the process parameters on the performance parameters. The output characteristics of ECG were studied by means of the Taguchi design based experiment with different

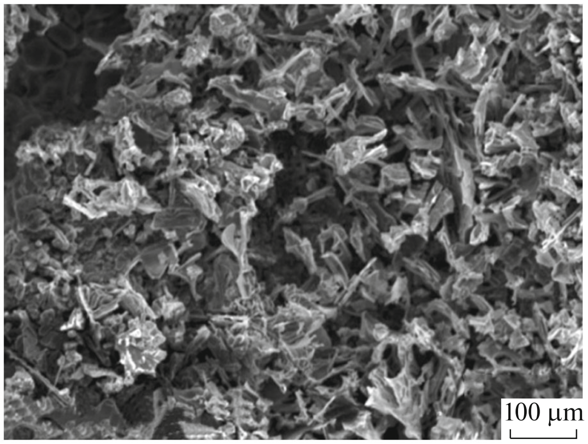

Fig. 2. Specimen machined with ECM [33].

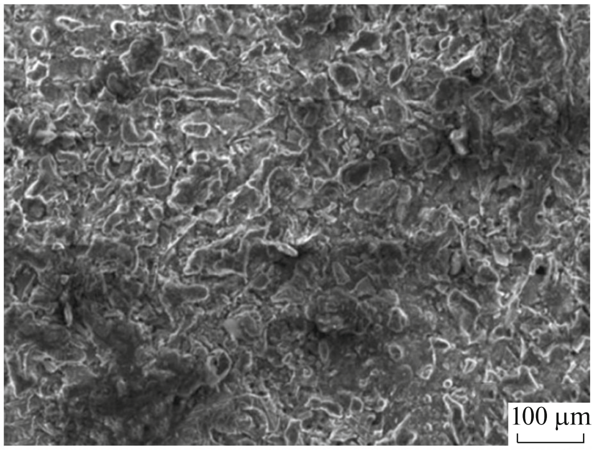

Fig. 3. Specimen machined with abrasive assisted ECM [33].

combinations of the process parameters. Hence the optimized parameters of ECG were obtained.

Electrochemical Micromachining

Electrochemical micromachining (ECMM) as a very promising future micromachining technique was discussed in [35]. The authors highlighted the influence of various electrochemical micromachining parameters like machining voltage, electrolyte concentration, pulse period and frequency on material removal rate, accuracy and surface finish in microscopic domain. According to their experimental study, the most effective values for micromachining parameters have been considered as 3 V machining voltage, 55 Hz frequency and 20 g/L electrolyte concentration that can enhance the accuracy with highest possible amount of material removal. Others [36] studied the characteristics of ECMM of AA6061 with 6 wt % graphite composite. In the latter study, the AA6061 reinforced with 6 wt % graphite composite was prepared by the stir casting technique. The particle size of graphite was 40 μm. During machining, $NaNO_3$ was used as the electrolyte solution. The effects of the process parameters such as voltage, electrolyte concentration, and frequency on the performance parameters such as MRR and ROC by using Taguchi L_{27} orthogonal array were studied and the results were subject to the analysis of variance (ANOVA). At the level of 9 V voltage, 20 g/L electrolyte concentration, and 55 Hz frequency, the maximum MRR of 0.495 mg/min was obtained. Similarly, at the level of 9 V voltage, 25 g/L electrolyte concentration, and 25 Hz frequency, the minimum ROC of 144.4 μm was obtained.

Electrochemical Drilling

Rao et al. [37] studied the machining characteristics of Al with 5 wt % boron carbide (B_4C) composite by electrochemical drilling. They used B_4C particles with a size of 30 μm and the AMMCs were prepared by the stir casting route. NaCl was used as the electrolyte solution. The developed mathematical model was based on Taguchi method and analyzed by ANOVA. They optimized the influences of machining parameters such as applied voltage, tool feed rate, and electrolyte concentration on the response parameter ROC. In that process, 0.5 mm inter-electrode gap, and 10 L/min electrolyte flow rate were kept constant while machining. It was observed that the response ROC enhanced with increasing the voltage and electrolyte concentration, but it reduced with increasing the tool feed rate. It was clear that the increase of parameters like voltage, tool feed rate, and electrolyte concentration by 65.44, 30.22, and 4.31%, respectively, increases ROC. The authors achieved the minimal ROC at the optimized level of 12 V voltage, 1 mm/min tool feed rate, and 10 g/L electrolyte concentration.

ECM OF VARIOUS ALUMINIUM MATRIX COMPOSITES

Silicon Carbide Reinforced Aluminium Matrix Composites

Senthilkumar et al. [38] developed the linear regression mathematical model by means of XLSTAT software. Taguchi L_{27} orthogonal array method with 54 trials was employed in the design of experiments. The samples were prepared in the composition of an aluminium alloy reinforced with varying SiC proportion of 5, 10, and 15 wt %. These composites were prepared by the stir casting method. NaCl was used as the electrolyte solution. While machining the composites of the cast aluminum alloy A356-SiC particles via ECM, the influence of the process parameters such as applied voltage, tool feed rate, electrolyte concentration, and percentage of reinforcement on the MRR was studied. Significant parameters and optimized levels were analyzed by ANOVA and the signal-to-noise ratio too. It was concluded that the effect of the process parameters on the MRR was evidenced by 14% applied voltage, 40% tool feed rate, and 26% electrolyte concentration. The maximum MRR 12.86 mg/min is achieved with optimal processing conditions such as 5 V applied voltage, 0.4 mm/min tool feed rate, 100 g/L electrolyte concentration and 5 wt % reinforcement. Also, they suggested the dispersion of SiC particles in the A356 matrix highly influenced the rate of the metal removal.

Pramanik et al. [39] reported that the MRR increases with higher such process parameters as applied voltage, tool feed rate, electrolyte concentration, and electrolyte flow rate. A higher machining current in the inter-electrode gap results from an increase in voltage and electrolyte concentration. When the gap between the tool and workpiece is reduced, the tool feed rate increases leading to a higher current density. Senthilkumar et al. [40] studied the electrochemical machining performance of Al-10 wt % SiC composites. The composites were prepared by the stir casting technique. They revealed that at low voltage applied in ECM, a high SR and a low MRR resulted. But an increased electrolyte flow rate resulted in the acceleration of the chemical reactions, accordingly increasing the MRR. When the applied voltage exceeds a certain limit and the electrolyte flow rate is constant, then more heat is produced that subsequently deteriorates the surface of the machined workpiece.

Senthilkumar et al. [41] optimized the machining parameters of Al-15 wt % SiC composites in electrochemical machining by using non-dominated sorting genetic algorithm-II method. Fabrication of LM 25 aluminium alloy reinforced with 15 wt % of SiC particles was done by means of the stir casting technique. The authors used sodium nitrate ($NaNO_3$) as the electrolyte solution. The design of the experiment through central composite design approach was established. In that study, the authors considered applied voltage, electrolyte concentration, tool feed rate and electrolyte flow rate as the input machining process parameters. They developed a statistical model for the MRR and the SR by using experimental data. The models were analyzed by ANOVA. Further, 4 and 5% errors were obtained in the MRR and the SR, respectively, when comparing the predicted and experimental results. The optimized values of the maximal MRR of 0.413 g/min and the minimal SR of Ra 2.172 μm were obtained at the following process parameters: 16 V applied voltage, 0.9 mm/min tool feed rate, 17 g/L electrolyte concentration, and 8 L/min electrolyte flow rate.

Hihara et al. [42] used ECM for machining Al-SiC composites using calomel as the tool material and aqueous $NaNO_3$ as the electrolyte solution. During the anodic dissolution, the matrix material was removed, whereas the inert SiC reinforced particles were removed by the electrolyte flow. The reduction in applied voltage and tool feed rate caused a high SR due to unsteady and non-homogeneous anodic dissolution. Moreover, as a result of a high current density caused by a higher tool feed rate and the existence of SiC particles in Al matrix, the pits on the workpiece surface were formed. In this process, hydrogen bubbles were produced, which obstructs the anodic dissolution, which, in turn, leads to the formation of the nodular work surface profile. A high electrolyte flow rate that aids in the removal of the hydrogen bubbles [43] and rotation of the tool at a particular speed, could prevent the nodular work surface profile. By means of controlling the current and tool feed rate perfectly, the required MRR could be achieved.

Boron Carbide (B_4C) Reinforced Aluminium Matrix Composites

On account of its high strength-to-weight ratio, greater wear resistance, high stiffness, toughness at the elevated temperature, B_4C is used for reinfor-cement, for example, in the automobile applications such as brake pads and brake rotor. Toptan et al. [44] reported on experimentation of ECM of aluminium reinforced with (2.5, 5.0, and 7.5 wt %) B_4C and studied the MRR. They developed a mathematical model for the MRR and applied ANOVA for the analysis. In that model, the mathematical relationship was established in between the input parameters such as applied voltage, tool feed rate, electrolyte concentration and percentage of reinforcement and the response parameter such as the MRR. They revealed that increasing the applied voltage leads to an increase of the machining current in the gap between the electrodes. Hence, it is attributed to increase the MRR. Similarly, an increase in the tool feed rate leads to the reduction in the gap between the electrodes and an increase in the current density in the inter-electrode gap. The resulted MRR was found to be high due to fast anodic dissolution. Moreover, the electrical conductivity of the electrolyte solution increased due to the increase in the concentration of electrolyte that enhances the number of ions in the gap between the anode and cathode. It may be attributed to increasing the machining current in the gap that tends to increase the MRR. However, the MRR decreased when the percentage of reinforcement in the metal matrix increased. Because of the poor electrical conductivity of reinforced materials, eventually decreases the electrical conductivity of Al-B_4C composites. It was reported that the highest MRR 0.966 g/min was obtained at the level of the following process parameters: 20 V applied voltage, 1.00 mm/min tool feed rate, 30 g/L electrolyte concentration, and 5 wt % B_4C reinforcement.

Rao et al. [45–47] developed the design of experiments by using Taguchi's L_{27} orthogonal array method for machining LM6 aluminium-B_4C composites. To determine the optimum level of the process parameters, the input parameters such as applied voltage, tool feed rate, electrolyte concentration, and percentage of reinforcement were correlated with the output responses such as the MRR, SR, and ROC. It was observed that the optimum level of the maximal MRR was achieved with the following processing conditions: applied voltage 20 V, tool feed rate 1.0 mm/min, electrolyte concentration 30 g/L, and percentage of reinforcement of B_4C 2.5 wt %. With the account of the signal-to-noise ratio, the MRR decreased only with an increase of the percentage of reinforcement of B_4C, but it increases with the rest of the parameters. It was reported that the contribution of the process parameters such as applied voltage, tool feed rate, electrolyte concentration, and percentage of reinforcement to the MRR is by 22.84, 52.67, 10.54, and 9.03%, respectively. The optimum level of the minimal SR was obtained at the following parameters: applied voltage 16 V, tool feed rate 1.0 mm/min, electrolyte concentration 30 g/L, and the percentage of reinforcement of B_4C 2.5%. The authors reported that the influence of the above process parameters on the SR is by 19.70, 29.13, 36.04, and 9.35%, respectively. Similarly, the optimum level of the minimum ROC was achieved at: applied voltage 12 V, tool feed rate 1.0 mm/min, electrolyte concentration 10 g/L, and percentage of reinforcement of B_4C 7.5 wt %. In [48], the authors optimized the influence of the process parameters on multi-response characteristics of Al-B_4C composites in ECM. They approached utility based on Taguchi L_{27} orthogonal array method for the design of experiments and outcomes were compared by using ANOVA technique. It was revealed that the tool feed rate is one of the most significant parameters to affect the multi-response parameters such as the MRR, SR, and ROC. It may be concluded with optimized parameters to achieve the maximum MRR and minimum SR and ROC are: 16 V applied voltage, 1.0 mm/min tool feed rate, 30 g/L electrolyte concentration, and 5 wt % of reinforcement.

Sankar et al. [48] studied the performance of ECM of AA7075-B_4C composites and optimized the responses of the MRR and SR by the response surface methodology, and then the result was analyzed by ANOVA. $NaNO_3$ was used as the electrolyte in this process. In that study, they considered current, voltage, and tool feed rate as input parameters. It was observed that such process parameters as voltage and tool feed rate highly influenced the MRR and SR. Therefore, the maximal MRR and the minimal SR was achieved at: 8 V applied voltage, 217 A current, and 0.3 mm/min tool feed rate.

Hybrid Boron Carbide (B_4C) and Graphite Reinforced Aluminium Matrix Composites

Sankar et al. in [49] also studied the machining characteristics of ECM of the hybrid AA6061-B_4C-graphite composite with and without abrasive silicon carbide particles. Also, they compared the abrasive assisted ECM with conventional ECM. In that study, the authors developed the mathematical model for the MRR in ECM and the parameters were optimized using the response surface methodology. It was observed that in the conventional ECM, due to poor electrical conductivity of reinforcement particles, the MRR was reduced, while the percentage of reinforcement in the aluminium alloy increased. But in the abrasive assisted ECM, the MRR increased and the SR reduced, when compared to ECM, due to the abrasive action of SiC particles in the electrolyte. They also revealed that the MRR increased with an increase in the tool feed rate. It was attributed to fast anodic dissolution that took place at a low inter-electrode gap with high current density. It was reported that ECM, assisted with SiC abrasive particles, shows greater performance than straight ECM. The MRR for the abrasive assisted ECM was higher than that with the straight ECM. Moreover, the SR with the abrasive assisted ECM was lower than that with the straight ECM. They also reported that the maximal MRR obtained with the abrasive assisted ECM and with the straight EMC were 0.064 and 0.063 g/min, respectively. Also, the optimized level of the process parameters in the abrasive assisted ECM were: 11 V applied voltage, 120 A current, 0.4 mm/min tool feed rate, and 10 wt % of B_4C reinforcement. Similarly, in straight ECM, the optimum conditions were: 14 V applied voltage, 240 A current, 0.4 mm/min tool feed rate, and 15 wt % of B_4C reinforcement.

Hybrid Alumina (Al_2O_3) and Silicon Carbide (SiC) Reinforced Aluminium Matrix Composites

Solaiyappan et al. [50] studied the performance of machining of AA6061 alloy with 10 wt % Al_2O_3 and 5 wt % SiC hybrid composites using straight ECM and that optimized by using hybrid fuzzy-artificial bee colony algorithm. They examined the influences of such process parameters as applied voltage, current, tool feed rate, electrolyte concentration, electrolyte flow rate and inter-electrode gap on such performance parameters as the MRR, SR, and ROC. The enhancing the current value and the tool feed rate results in the increase of the MRR and ROC, while the SR decreases. It was due to increasing the current density in the gap between the anode and cathode at the time of increasing the current. At a low inter-electrode gap, the MRR increased but the SR decreased initially but after a while it increased. At 0.1 mm inter-electrode gap, the maximal MRR and the minimal SR and ROC were achieved. The optimized response values for the MRR, SR, and ROC were: 0.813 g/min, Ra 1.23 μm, and 0.142 mm, respectively.

CONCLUSIONS

The machining characteristics of ECM on the AMMCs have been reported in this survey paper. In ECM, an increase of such process parameters as applied voltage, tool feed rate, electrolyte concentration, and flow rate leads to an increase of the MRR, but the latter response parameter reduces with the addition of reinforcement materials in AMMCs. The ROC increased with higher voltage and electrolyte concentration, however, it decreased with an increased tool feed rate. The SR decreased with an increase of current, voltage, and tool feed rate.

REFERENCES

1. Pal, T.K., *Mater. Manuf. Process.*, 2005, vol. 20, no. 4, pp. 717–726.

2. Bandyopadhyay, N.R., Ghosh, S. and Basumallick, A., *Mater. Manuf. Process.*, 2007, vol. 22, no. 6, pp. 679–682.
3. Ding, X., Liew, W.Y.H. and Liu, X.D., *Wear*, 2005, vol. 259, pp. 1225–1234.
4. Hynes, N.R.J., Kumar, R., Tharmaraj, R. and Velu, P.S., *AIP Conf. Proc.*, 2016, vol. 1728, pp. 1–5.
5. Sahin, Y., Kok, M. and Celik, H., *J. Mater. Process. Technol.*, 2002, vol. 128, pp. 280–291.
6. Chandrasekaran, H. and Johansson, J.O., *CIRP Annu. Manuf. Tech.*, 1997, vol. 46, no. 1, pp. 493–496.
7. Tomac, N., Tonnessen, K. and Rasch, F.O., *CIRP Annu. Manuf. Tech.*, 1992, vol. 41, no. 1, pp. 55–58.
8. Cronjager, L. and Meister, D., *CIRP Annu. Manuf. Tech.*, 1992, vol. 41, no. 1, pp. 63–68.
9. Avevor, Y., Moufki, A. and Nouari, M., *Proc. CIRP*, 2017, vol. 58, pp. 539–542.
10. Hung, N.P., Boey, F.Y.C. and Khor, K.A., *J. Mater. Process. Technol.*, 1995, vol. 48, nos. 1–4, pp. 291–297.
11. Zhang, Z., Zhu, D., Qu, N. and Wang, M., *Microsyst. Technol.*, 2007, vol. 13, no. 7, pp. 607–612.
12. Ebeid, S.J., Hewidy, M.S., El-Taweel, T.A. and Youssef, A.H., *J. Mater. Process. Technol.*, 2004, vol. 149, nos. 1–3, pp. 432–438.
13. Neto, J.C.D.S., Silva, E.M.D., and Silva, M.B.D., *J. Mater. Process. Technol.*, 2006, vol. 179, nos. 1–3, pp. 92–96.
14. Zhu, D. and Xu, H.Y., *J. Mater. Process. Technol.*, 2002, vol. 129, nos. 1–3, pp. 15–18.
15. Davydov, A.D., Kabanova, T.B., and Volgin, V.M., *Russ. J. Electrochem.*, 2017, vol. 53, no. 9, pp. 941–965.
16. Kozak, J., *J. Mater. Process. Technol.*, 1998, vol. 76, nos. 1–3, pp. 170–175.
17. Rajurkar, K.P., Zhu, D., McGeough, J.A., Kozak, J., and Silva, A.D., *CIRP Annu. Manuf. Technol.*, 1999, vol. 48, no. 2, pp. 567–579.
18. McGeough, J.A., *Principles of Electrochemical Machining*, London: Chapman and Hall, 1974.
19. Lohrengel, M.M., Rataj, K.P., and Munninghoff, T., *Electrochim. Acta*, 2016, vol. 201, pp. 348–353.
20. Xu, Z., Chen, X., Zhou, Z., Qin, P., and Zhu, D., *Proc. CIRP*, 2016, vol. 42, pp. 125–130.
21. Singh, T. and Dvivedi, A., *Int. J. Mach. Tool Manuf.*, 2016, vol. 105, pp. 1–13.
22. Hocheng, H., Sun, Y.H., Lin, S.C., and Kao, P.S., *J. Mater. Process. Technol.*, 2003, vol. 140, nos. 1–3, pp. 264–268.
23. Wilson, J.F., *Practice and Theory of Electrochemical Machining*, New York: Wiley, 1971.
24. Rajurkar, K.P., Sundaram, M.M., and Malshe, A.P., *Proc. CIRP*, 2013, vol. 6, pp. 13–26.
25. Neergat, M. and Weisbrod, K.R., *Corros. Sci.*, 2011, vol. 53, no. 12, pp. 3983–3990.
26. Hihara, L.H. and Panquites, P., US Patent 6110351, 2000.
27. Westley, J.A., Atkinson, J. and Duffield, A., *J. Mater. Process. Technol.*, 2004, vol. 149, nos. 1–3, pp. 384–392.
28. Chunhua, S., Di, Z., Zhiyong, L. and Lei, W., *Finite Elem. Anal. Des.*, 2006, vol. 43, no. 2, pp. 168–172.
29. Swain, A.K., Sundaram, M.M., and Rajurkar, K.P., *J. Manuf. Process.*, 2012, vol. 14, no. 2, pp. 150–159.
30. Sen, M. and Shan, H.S., *Int. J. Mach. Tool Manuf.*, 2005, vol. 45, no. 15, pp. 1706–1716.
31. Krishnaiah Chetty, O.V., and Radhakrishnan, V.A., *Int. J. Mach. Tool Des. Res.*, 1981, vol. 21, no. 1, pp. 57–69.
32. Konig, W. and Linderlauf, P., *CIRP Annu. Manuf. Tech.*, 1978, vol. 27, no. 1, pp. 97–100.
33. Sankar, M., Gnanavelbabu, A., and Rajkumar, K., *Proc. Eng.*, 2014, vol. 97, pp. 381–389.
34. Goswami, R.N., Mitra, S. and Sarkar, S., *Int. J. Adv. Manuf. Technol.*, 2009, vol. 40, pp. 729–741.
35. Bhattacharyya, B., Malapati, M., and Munda, J., *J. Mater. Process. Technol.*, 2005, vol. 169, pp. 485–492.
36. Satishkumar, P., Dharmalingam, S., Raja, K., Lingadurai, K., et al., *Int. J. Chem. Tech. Res.*, 2015, vol. 7, no. 1, pp. 203–211.
37. Rao, S.R., Padmanabhan, G., Mahesh, N.K. and Rukesh, R.A., *Proc. Eng.*, 2014, vol. 97, pp. 1004–1011.
38. Senthilkumar, K.L., Sivasubramanian, R., and Kalaiselvan, K., *Port. Electrochim. Acta*, 2009, vol. 27, no. 4, pp. 477–486.
39. Pramanik, A., *Int. J. Mach. Tool Manuf.*, 2014, vol. 86, pp. 44–61.
40. Senthilkumar, C., Ganesan, G., and Karthikeyan, R., *Int. J. Adv. Manuf. Technol.*, 2009, vol. 43, pp. 256–263.
41. Senthilkumar, C., Ganesan, G., and Karthikeyan, R., *Trans. Nonferrous Met. Soc. China*, 2011, vol. 2, pp. 2294–2300.
42. Hihara, L.H. and Panquites, P., *Abrasive Grinding Mag.*, 2003, vol. 12, pp. 12–17.
43. Rajurkar, K.P. and Hewidy, M.S., *J. Mech. Work. Technol.*, 1988, vol. 17, pp. 315–324.
44. Toptan, F., Kilicarslan, A., and Kertil, I., *Mater. Sci. Forum*, 2010, vol. 192, pp. 636–637.
45. Rao, S.R. and Padmanabhan, G., *Arch. Appl. Sci. Res.*, 2012, vol. 4, no. 4, pp. 1844–1849.
46. Rao, S.R. and Padmanabhan, G., *Int. J. Appl. Sci. Eng.*, 2014, vol. 12, no. 2, pp. 87–97.
47. Rao, S.R. and Padmanabhan, G., *J. Eng. Sci. Technol.*, 2015, vol. 10, no. 1, pp. 81–96.
48. Sankar, M., Gnanavelbabu, A. and Baskaran, R., *Appl. Mech. Mater.*, 2014, vol. 606, pp. 193–197.
49. Sankar, M., Baskaran, R., Rajkumar, K., and Gnanavelbabu, A., *Appl. Mech. Mater.*, 2014, vol. 591, pp. 89–93.
50. Solaiyappan, A., Mani, K., and Gopalan, V., *Jordan J. Mech. Ind. Eng.*, 2014, vol. 8, no. 5, pp. 323–331.